CHAPTER 5:

TOPOGRAPHIC MAPPING OF VOICE CROSSMODAL PLASTICITY

Introduction

Sensory substitution neural imaging studies have focused on the presence of crossmodal plasticity, and the functional association of the task and neural region activated. No sensory substitution study has investigated the mapping of visual space via sensory substitution to a spatiotopic or "retinotopic" map. Retinotopic mapping processes adjacent regions in visual space by neighboring regions of cortex. Vision has a retinotopic map (detailed below) that is based on the 2D spatial luminance-detection of the two retinas. The basic principle of the visual retinotopic mapping is the representation of the contralateral visual field in each hemisphere (*i.e.,* left visual field is processed by the right primary visual cortex, and vice versa). This chapter will focus on an fMRI experiment determining whether the same contralateral mapping of visual space occurs with vOICe spatial perception. This is an intriguing question, because in the A-V type of sensory-substitution device (such as the vOICe), the auditory inputs after appropriate training may systematically induce early visual cortical activation (as reviewed in Chapter 1 and 4). Yet, which neural pathway and/or multisensory plasticity enable it, is not very well understood. The empirical data answering the spatial mapping of this crossmodal plasticity will shed light on the underlying neural pathways responsible for multisensory plasticity with the SS device/training.

Investigation of the spatial mapping to neural activation of SS may show that like vision, it is retinotopically mapped. Visual mapping of space begins at the retinal level

(Figure 5.1). Each retina detects an inverted image of both the left and right visual field, which is then separated into left and right visual fields at the optic chiasm. The left visual field fibers merge from both eyes and exit right of the optic chiasm, and vice versa. The fibers then continue to the thalamus' lateral geniculate nucleus (LGN) and onto primary visual cortex in the occipital lobe. Primary visual cortex or V1 spatially maps the hemifield on the cortical surface, as is elegantly shown in Tootell *et al.*'s mapping of the macaque monkey (Figure 5.2) (Tootell, Silverman, Switkes, & De Valois, 1982). Tootell and colleagues used a c-labeled deoxy-d-glucose prior to exposure of the animal to the visual target pattern (Figure 5.2 A). The chemical label could then be used to stain recently activated neural cells and therefore show the pattern of activation on the cortex itself. Their results (Figure 5.2 B) show the incredible fidelity of the retinotopic map to the original image with the following modification – that is, the map is logarithmically magnified at the foveal region relative to the periphery. More recently, fMRI imaging has been used to generate detailed retinotopic maps in humans for not only V1 but also V2, and V3 among others (Kolster, Peeters, & Orban, 2010; M. Sereno et al., 1995; M. I. Sereno, Pitzalis, & Martinez, 2001). It is useful to note that the sharpness of the contralateral mapping (*i.e.,* left hemisphere to right visual field) decreases as information progresses from V1 to higher visual cortices. Consequently, extrastriate regions represent an increasing amount of the ipsilateral visual field. For example, Tootell *et al.* determined in 1995 that MT neurons responded to visual stimuli up to 20 degrees into the ipsilateral receptive field (Tootell et al., 1995).

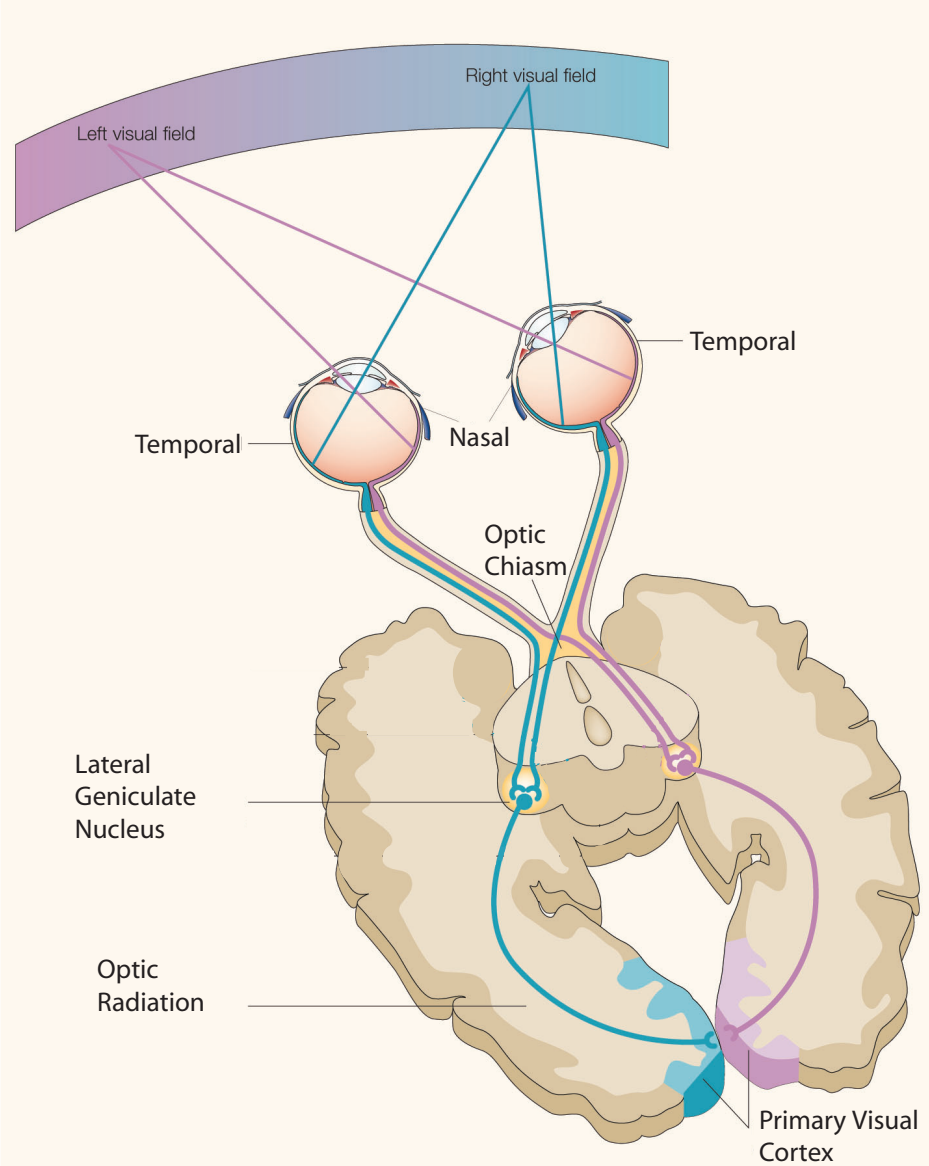

Figure 5.1. Diagram of the mapping of visual space to cortical activation. This diagram indicates the mapping of the left and right visual fields from the retina, through the optic chiasm and lateral geniculate nucleus to the primary visual cortex (V1). It is accomplished by the nasal part of each of the retinae projects to the contralateral, whereas the temporal part of it projects to the ipsilateral visual cortices (Hannula, Simons, & Cohen, 2005).

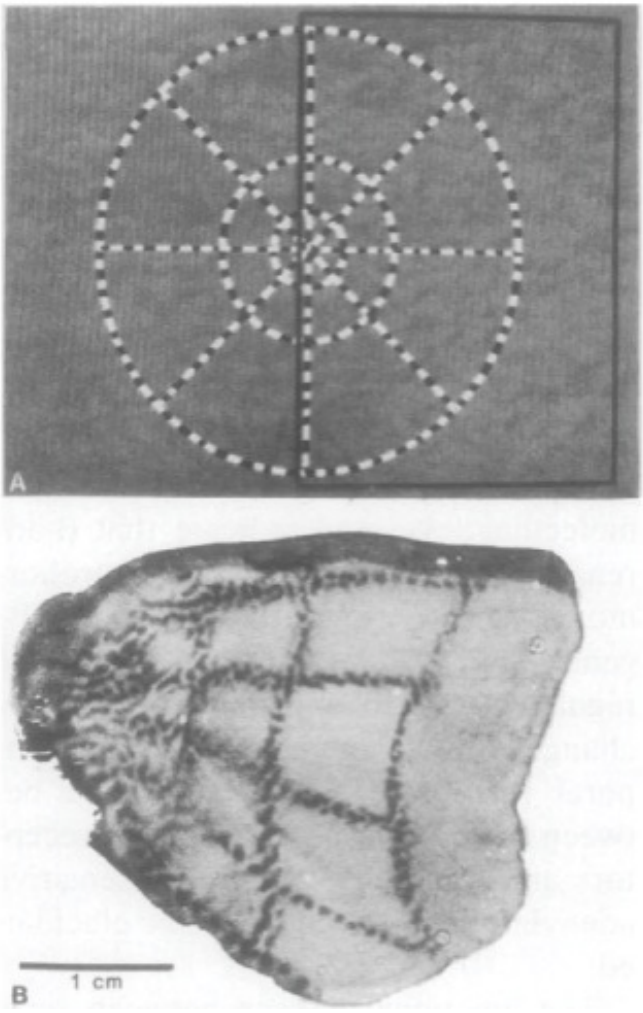

Figure 5.2. Retinotopic mapping of macaque striate cortex. Tootell and colleagues demonstrate the retinotopic mapping of visual space onto the primary visual cortex with a deoxyglucose analysis method (Tootell, et al., 1982). The image of visual cortex (image B) shows half of the pattern visually presented to the monkey (image A), indicating the mapping of half visual space to neural activation (indicated by dark patches of cortex) in the contralateral hemisphere and the mapping of neighboring spatial regions to adjacent regions of visual cortex. (Tootell, et al., 1982)

Visual retinotopic maps are plastic, and can be modified by visual deprivation. Several studies have investigated the implications to retinal mapping when a cortical lesion occurs, whether via stroke or surgical intervention. A patient with the loss of one visual field due to stroke in the left hemisphere of the occipital cortex was able to remap both visual fields onto the visual regions of the intact occipital lobe, including V1 (Henriksson, Raninen, Nasanen, Hyvarinen, & Vanni, 2007). Further, a participant with a right hemispherectomy (removal of the right hemisphere) due to epilepsy had visual activation in the left V3 and the left V5 in response to stimuli in the blind visual field (left side); thus the projection was plastically re-organized ipsilaterally (Bittar, Ptito, Faubert, Dumoulin, & Ptito, 1999). Interestingly, this right hemispherectomy participant also experienced blind sight (unconscious visual perception), whereas the two other hemispherectomy participants in the study did not have visual activation from their blind hemifield or blind sight.

Visual retinotopic maps can also be modified by altered visual perception via prism glasses (detailed prism discussion in Chapter 4 discussion). Sugita found that the primate visual cortex became sensitive to the ipsilateral visual field after wearing left-right reversing prisms for one and a half months (Sugita, 1996). Further, Miyauchi and colleagues used fMRI imaging in humans wearing left-right reversing glasses to show that V1 and extrastriate visual regions became sensitive to ipsilateral visual stimuli (Miyauchi et al., 2004). These remapping results are valuable indicators of the plasticity of spatial maps in early visual regions.

Other investigations have studied the impact of retinal diseases on cortical maps, in particular investigating whether remapping occurs in the de-afferented cortex. Baseler

et al. studied the responsiveness of the cortical region that represents the all-cone foveola in congenital rod monochromats (colorblind people with nearly no cone receptor function) (Baseler et al., 2002). Baseler and colleagues determined that in rod-monochromats, remapping occurred in the foveola cortical region. The foveola now responded to rod-dominated retinal regions. The reorganization of de-afferented cortex of late-onset retinal diseases is less clear. In particular, Baseler and colleagues argued in 2011 that remapping does not occur in humans with bilateral central vision damage from Age-Related Macular Degeneration (AMD) (Baseler et al., 2011).

Even blind individuals have been shown to have spatiotopic maps of perception in visual regions. It was reported that a visually-impaired participant was able to activate normally foveal visual areas by Braille reading, while normally peripheral visual areas were activated by his remaining low vision (Cheung, Fang, He, & Legge, 2009). Further, Milne *et al.* were able to map azimuth of echo-locations on the visual cortex in an early blind echolocation expert in a way that is similar to the visual spatiotopic map (Milne, Goodale, & Thaler, 2013). Therefore, it is plausible that sensory substitution could generate a spatiotopic map in visual cortex.

This chapter will report experiments that investigate whether crossmodal plasticity with vOICe can be spatiotopically organized. The main fMRI task before and after training on vOICe will ask participants to localize a dot on the left or right, with the dots conveyed via vOICe sounds or via images. The mapping of visual space via vOICe to visual activation will then be determined by the comparison of the neural activation from the left dot and the right dot. Both sighted and blind individuals will participate in

the task, and thereby indicate whether the spatial mapping is different among these participant groups.

Methods

Participants

Participant information is detailed in Chapter 4 methods (p. 130). The same participants and scan sessions were used for Chapter 5 fMRI data collection as were used in Chapter 4. Chapter 5 analyzes the fMRI data results for two localization tasks not detailed in Chapter 4.

Experiment Design

The Chapter 4 methods describe the experimental design for both Chapter 4 and 5. Figure 4.01 also details the experimental layout for both Chapter 4 and 5.

vOICe Training Procedure

Participant training procedure on the vOICe device is explained in Chapter 4 methods, and in Appendix B part 1.

fMRI Tasks

Overview

Six separate tasks were performed in each fMRI scanning session. The four tasks relevant to the automaticity of vOICe processing are described in Chapter 4's methods. The remaining 2 tasks relevant to the mapping of vOICe from visual space to visual activation (*i.e.,* Chapter 5) are explained below.

vOICe Dot Localization

To perform the vOICe localization task, participants are asked to fixate on a cross in the center of the field of view, and listen to an image of white dot encoded into sound with vOICe play twice (Figure 5.3). The white dot can be located in the left visual field (*i.e.,* on the left side) or in the right visual field (*i.e.,* on the right side). Participants are asked to press 1 if the dot is located on the left, and 2 if the dot is located on the right. Participants after training are told that the sound is vOICe, and that this task is like the localization performed with vOICe during training. Before training, participants are typically told to press 1 if they hear a high-pitched sound on the left, and to press 2 if they hear it on the right. The vOICe sounds paired with the correct responses are also indicated before the participants start the task in both pre-training and post-training sessions. The participant's eye movements were recorded in both sessions to verify that participants move their gaze minimally, therefore not significantly modifying their spatial frame of reference. Participants performed 100 total trials of vOICe localization before and after training; 50 trials for the left-sided dot, and 50 trials for the right-sided dot, in randomized order.

Vision Dot Localization

To perform the visual localization task, participants were asked to fix their gaze on a central cross and locate a white dot presented on the left or right of the image center (Figure 5.4). Participants responded by pressing 1 if the white dot was on the left, and 2 if the white dot was on the right. The participant's eye movements were recorded in both sessions to verify that participants move their gaze minimally, therefore not significantly modifying their spatial frame of reference. Participants performed 100 total trials of

visual localization before and after training; 50 trials for the left-sided dot, and 50 trials for the right-sided dot, in randomized order.

Blind Participant Tasks

Blind participants performed the vOICe dot localization task, but not the vision dot localization task. Instructions for the vOICe dot localization task were read aloud by the Macintosh Computer Speech utility and recorded by QuickTime into an audio mov file. These mov files were converted into wav files, and loaded into MATLAB to be played at the beginning of the experiment. Eye movements were not recorded for blind participants. All other elements of the experimental design were the same for the blind participants, including the vOICe training.

fMRI Data Acquisition, Preprocessing, and Postprocessing (Statistical Analysis)

fMRI data collection parameters, and data pre- and post-processing details are in the Chapter 4 methods.

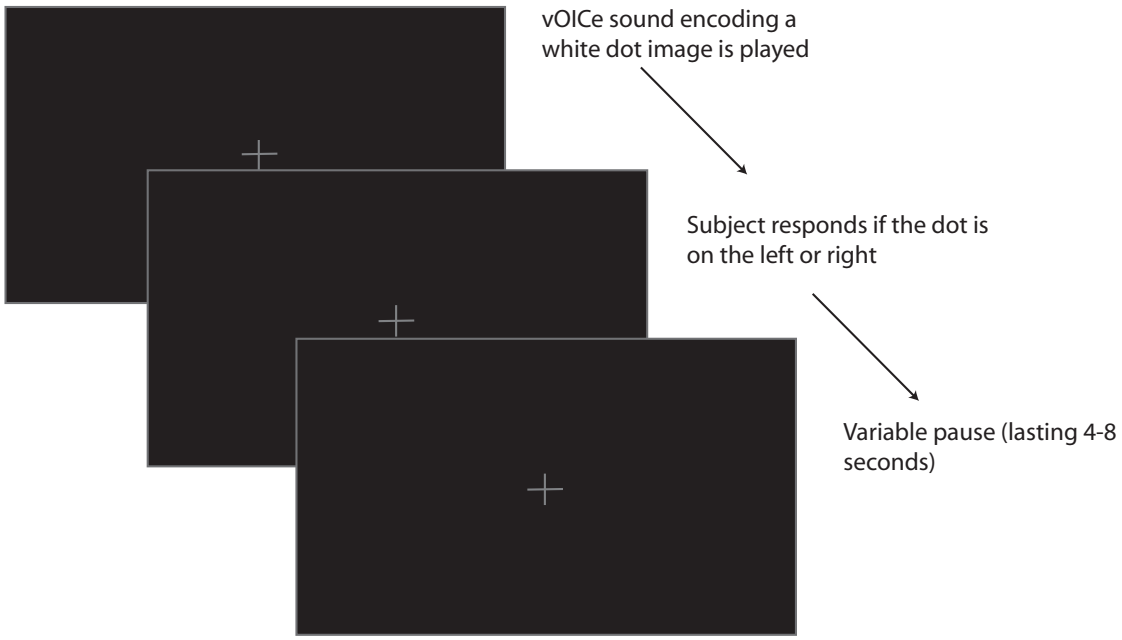

Figure 5.3. fMRI experiment diagram of the vOICe localization task. Participants localized a white dot on black background encoded into vOICe on the left or right. They responded after the sound finished if the dot was on the left by pressing 1, and the right by pressing 2. One hundred localization trials were performed, with 50 left dot trials and 50 right dot trials.

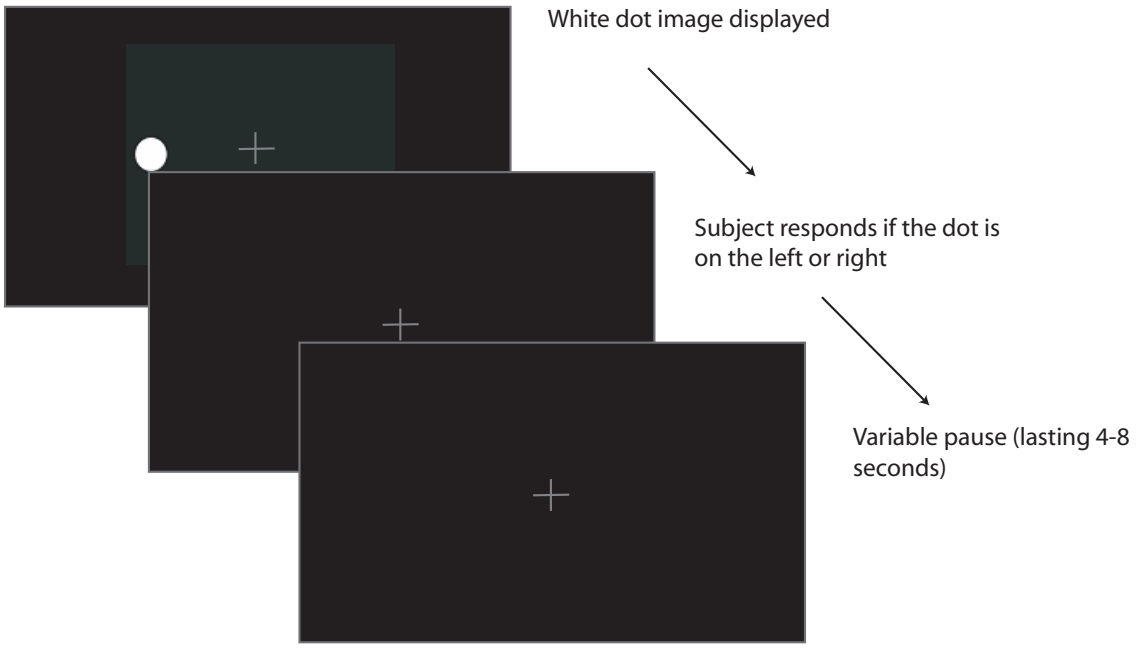

Figure 5.4. fMRI experiment diagram of the vision localization task. Participants localized a white dot on black background on the left or right with vision. They responded after the image disappeared if the dot was on the left by pressing 1, and the right by pressing 2. One hundred localization trials were performed, with 50 left dot trials and 50 right dot trials.

Results

Sighted Participant Neural Imaging Results

The contrast of vOICe localization [Right – Left] post-training and [Left – Right] post-training were used to investigate the spatial mapping of vOICe perception in 10 sighted participants (Note: [Right – Left location] and [Right – Left] will be used to indicate that the left dot location scans were subtracted from the right dot location scans and vice versa; the word(s) *post-training* after the brackets indicates that all the scans were all derived from the post-vOICe-training scan session). If a contralateral mapping exists, [Right – Left] will generate visual activation in the left hemisphere and [Left – Right] in the right hemisphere. Figure 5.6 and Table 5.1 show the results for this contrast. For the [Right – Left] vOICe contrast, significant activation was found in Brodmann Areas (BA) 19, 39, and 22 in the left hemisphere among other regions. A small volume correction for BA 19 yielded a pvalue less than 0.05, when a sphere of 10 mm radius was used (Table 5.1). For the contrast of [Left – Right] post training vOICe (Table 5.1), only the cingulate gyrus was activated. Therefore, the sighted participants had a contralateral mapping from a *right* dot in visual space to visual activation in *left* hemisphere of the brain. This contralateral mapping from space to visual neural activation via vOICe sound mimics the contralateral mapping in traditional visual perception.

In order to have a direct comparison of vOICe localization to vision localization, a vision control task was also performed by participants before and after training on the vOICe device. The vision contrast of [Right – Left] post-training and [Left – Right] post-training are shown in Figure 5.6 and Table 5.2. The [Right – Left] post-training in vision

had significant activation in BA 19 in the left hemisphere and BA 39 in the right hemisphere among other regions. A small volume correction of BA 19 and BA 39 yielded pvalues below 0.05 for a sphere of 10 mm radius (Table 5.2). Nearly all of the neural activation in early visual regions (*i.e.* BA 17, 18, or 19) occurred in the left hemisphere, therefore indicating a largely contralateral mapping from visual space to neural activation (as expected). In a similar pattern to the vOICe localization results, the vision [Left – Right] post-training did not have any significant activation in visual or any other brain regions. This strange dominance of the right over the left visual field visual activation could have several possible causes. The repetition and simiplicity of the task that could decrease visual activation (particularly because the scans studied above were in the second fMRI session) therefore make inter-hemisphere differences more apparent. It is also possible that vOICe training reduced the strength of visual activation via competition with the crossmodal visual activation as proposed in Chapter 4.

Sighted Participant Neural Imaging Correlation with Subjective Reports

All participants filled out a questionaire following the experiment (full questionaire in Appendix C). The results for a few questions relevant to the localization experiment are plotted in Figure 5.7. The first plot indicates that most participants did not visually imagine the dot while performing the localization task with the vOICe, and those that did have visual imagining only had them following the sound (Figure 5.7A). The scans used for the fMRI contrasts are only during the sound duration; therefore, any visual imaginings following the sound are not relevant for the fMRI analysis of the vOICe localization task. Therefore, this questionaire data indicates that visualization did not play an important role in the generation of visual activation with vOICe localization.

The second plot presented (Figure 5.7B) shows that all sighted participants attempted to fixate their gaze during the vOICe localization task. This is particularly important because a wandering gaze is not only distracting, but may also alter the participant's visual frame of reference while performing the vOICe localization task, and therefore alter their spatial mapping of vOICe. This result critically shows that any visual wandering was minimized by active participant fixation during the localization task.

An fMRI covariate analysis was used to further tie the visual activation during the localization task with vOICe via vOICe performance during training. Two covariates were used for functional vOICe localization performance during training: The slope (improvement) and intercept (initial performance) of the vOICe localization inaccuracy *vs.* training time plot (Figure 4.07 and Figure 4.08). The covariates used are the same covariates as were used in Chapter 4 on the distraction vOICe task. The covariate procedure is detailed in Chapter 4 methods, and the individual covariate details are in the Chapter 4 results. The slope covariate showed a medial frontal area correlated with improvement at localization, and the intercept covariate showed that BA 19 ($p < 0.05$, small volume corrected) correlated with initial localization performance (Table 5.3). The visual activation result for the localization intercept covariate is interesting, and verifies that the visual activation in the vOICe localization task is likely due to vOICe interpretation. The correlation with initial performance (intercept) rather than improvement (slope) may be due to the fact that the localization task is quite intuitive from the beginning, and therefore the intuitive existing crossmodal correspondences play a strong role in the visual activation from vOICe.

A

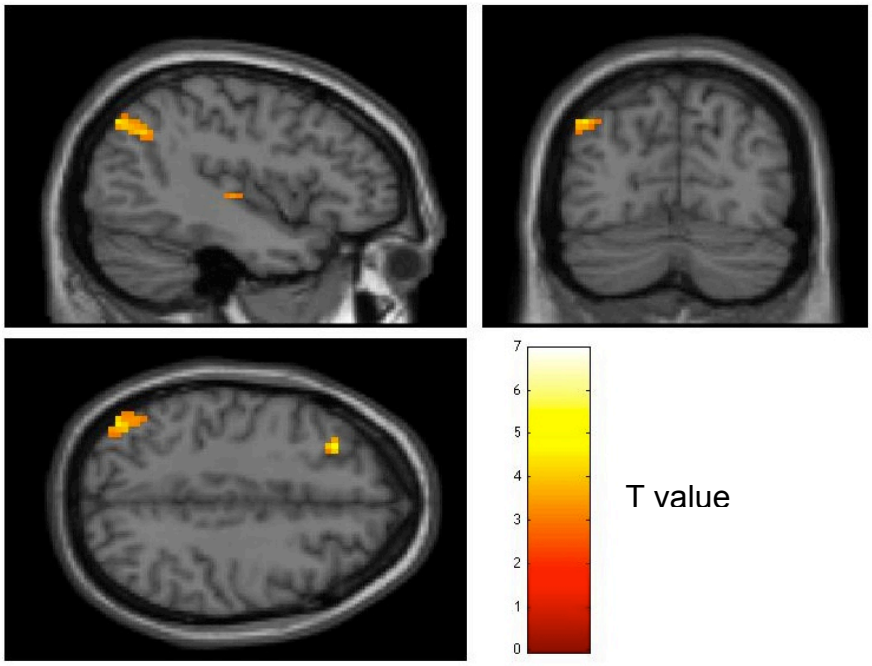

B

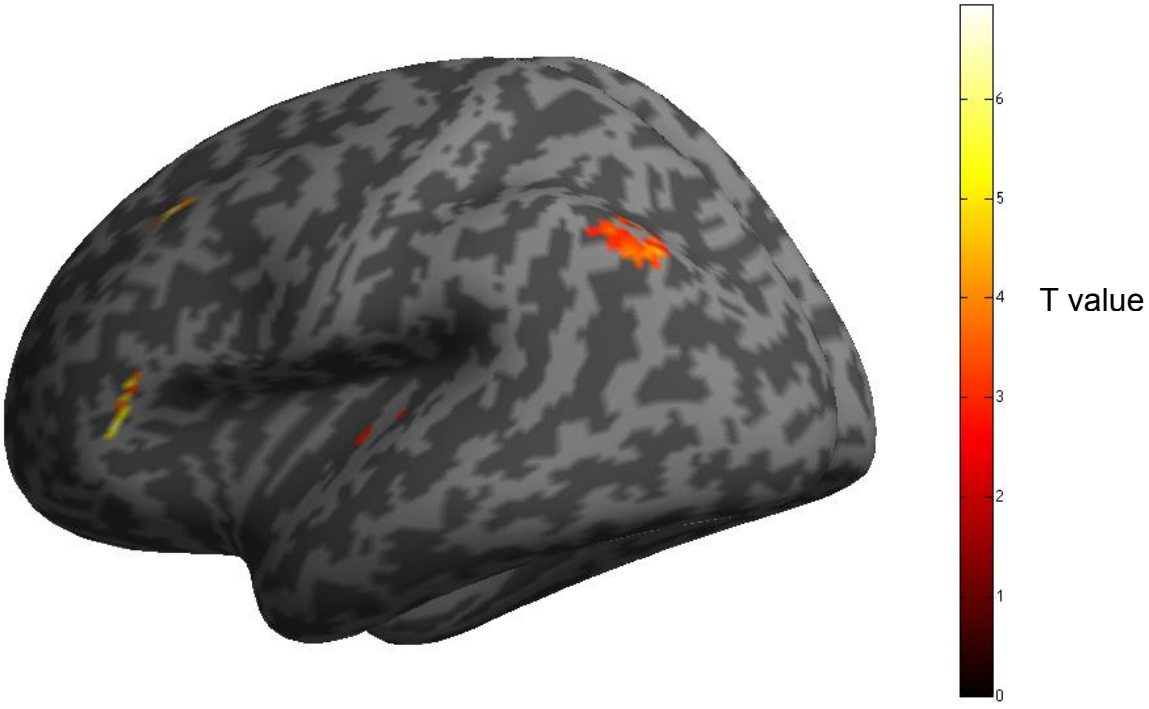

Figure 5.5. fMRI imaging results: vOICe dot [Right – Left location] post-scan in sighted participants. The neural imaging result is displayed for the post-vOICe-training right dot in contrast to thr post-vOICe-training left dot both presented in vOICe with sighted participants ($N = 10$). Imaging data presented is $p < 0.009$ uncorrected and clusters of 10 voxels or more; further correction for multiple comparisons is shown in Table 5.1. Methods for fMRI data display are in the Chapter 4 methods.

Sighted Participants (*N* = 10)						
Region	BA	Side	*x*	*y*	*z*	p_{uncorr}
vOICe Dot Post [Right – Left]						
Superior Frontal Gyrus	8	L	−30	29	46	0.000
Inferior Frontal Gyrus	45	L	−48	26	1	0.000
Precuneus	19	L	−42	−73	43	0.001
- small volume-corrected peak						0.043*
Angular Gyrus	39	L	−42	−61	37	0.001
- small volume-corrected peak						0.056*
Medial Frontal Gyrus	10	R	9	47	10	0.001
Superior Temporal Gyrus	22	L	−48	−7	1	0.004
- small volume-corrected peak						0.112*
Insula	13	L	−42	−19	1	0.005
vOICe Dot Post [Left – Right]						
Cingulate Gyrus	32	L	−15	20	31	0.000
Cingulate Gyrus	24	L	−9	-4	28	0.000
Cingulate Gyrus	24	L	−15	−1	34	0.001

Table 5.1. fMRI imaging results: vOICe dot post-scan sighted participants. Imaging results for sighted participants when comparing the post-training left dot and the post-training right dot in vOICe ($N = 10$). All regions were limited to $p < 0.009$ uncorrected and 10 voxel cluster threshold. The small volume correction was for a sphere of 10 millimeters radius around the cluster center, and the pvalue shown (indicated by asterisk, *i.e.*, *) is for the peak level FWE-corrected. Brodmann Area localization was performed

on the talaraich client for nearest grey matter. Any clusters without nearest grey matter within +/– 5 mm are not included.

A

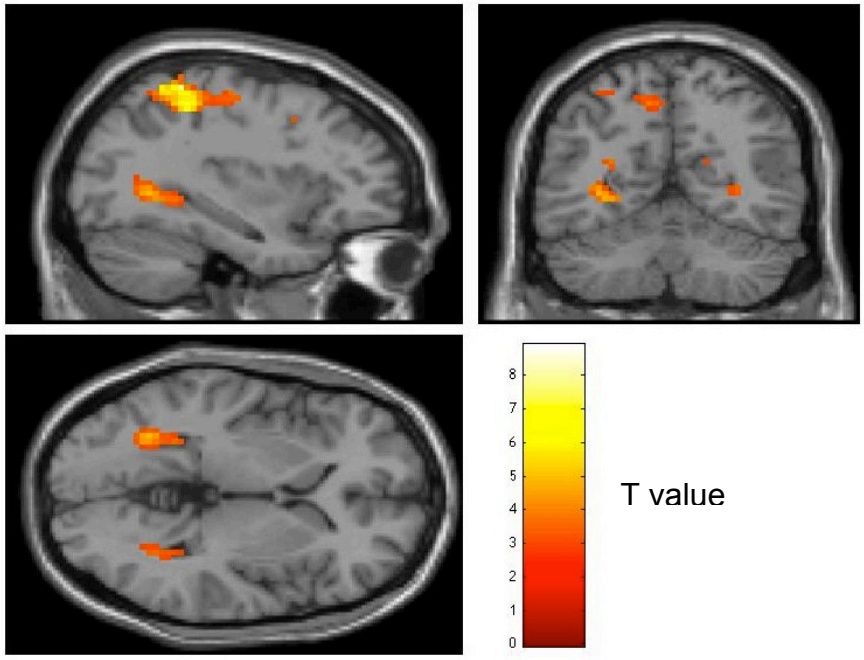

B

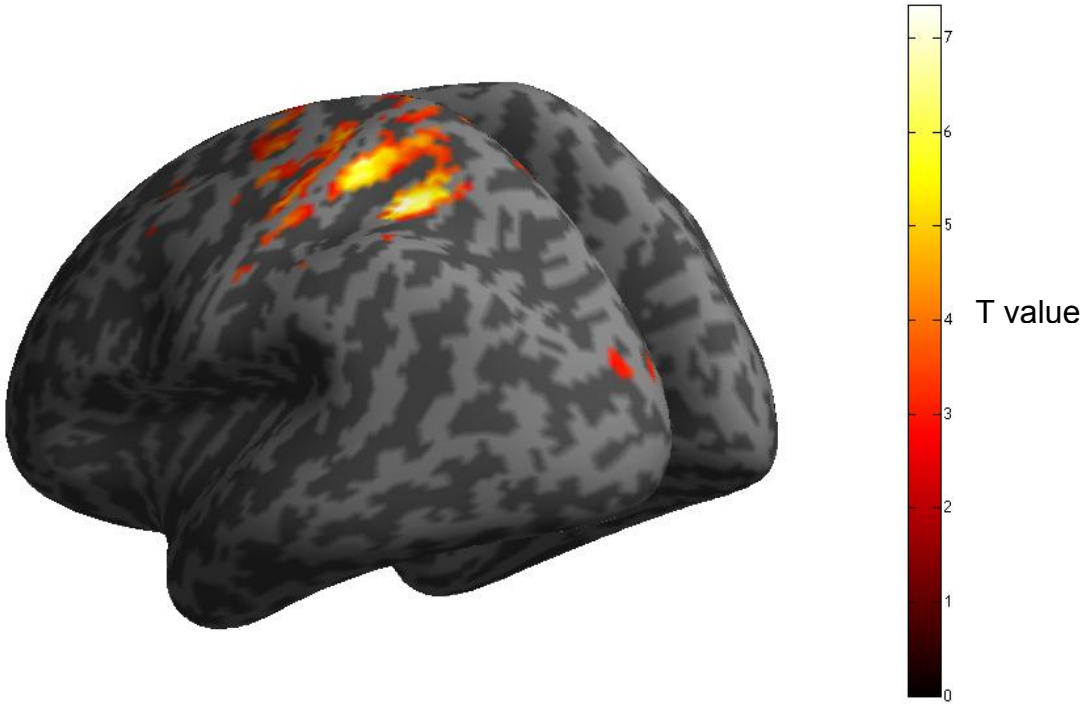

Figure 5.6. fMRI imaging results: Vision dot [Right – Left location] post-scan in sighted participants. The neural imaging result is displayed for the post-vOICe-training right dot in contrast to the post-vOICe-training left dot, both presented in vision with sighted participants ($N = 10$). Imaging data presented is $p < 0.009$ uncorrected and clusters of 10 voxels or more; further correction for multiple comparisons is shown in Table 5.2. Methods for fMRI data display are in the Chapter 4 methods.

Sighted Participants (*N* = 10)						
Region	BA	Side	*x*	*y*	*z*	p_{uncorr}
Vision Dot Post [Right – Left]						
Inferior Parietal Lobule	40	L	−36	−43	52	0.000
Postcentral Gyrus	5	L	−36	−43	61	0.000
Superior Parietal Lobule	7	L	−33	−52	61	0.000
Lingual Gyrus	19	L	−33	−58	1	0.000
- small volume-corrected peak						0.016*
Parahippocampal Gyrus	19	L	−30	−46	-2	0.001
- small volume-corrected peak						0.029*
Angular Gyrus	39	R	48	−70	28	0.002
- small volume-corrected peak						0.039*
Posterior Cingulate	31	L	−27	−58	19	0.003
Cuneus	18	L	−18	−82	22	0.003
Cuneus	18	L	−15	−91	16	0.005
Middle Frontal Gyrus	6	L	−27	11	43	0.003
Cingulate Gyrus	24	R	9	2	46	0.003
Parahippocampal Gyrus	19	R	33	−55	1	0.004
Cingulate Gyrus	31	R	21	−46	22	0.005
Vision Dot Post [Left – Right]						
No significant activation						

Table 5.2. fMRI imaging results: Vision dot [Right – Left location] post-scan sighted participants. Imaging results for sighted participants when comparing the post-training left dot and the post-training right dot in vision ($N = 10$). All regions were limited to $p < 0.009$ uncorrected and 10 voxel cluster threshold. The small volume correction was for a sphere of 10 millimeter radius around the cluster center, and the pvalue shown (indicated by asterisk, *i.e.*, *) is for the peak level FWE-corrected. Brodmann Area localization was performed on the talaraich client for nearest grey matter. Any clusters without nearest grey matter within +/– 5 mm are not included.

A

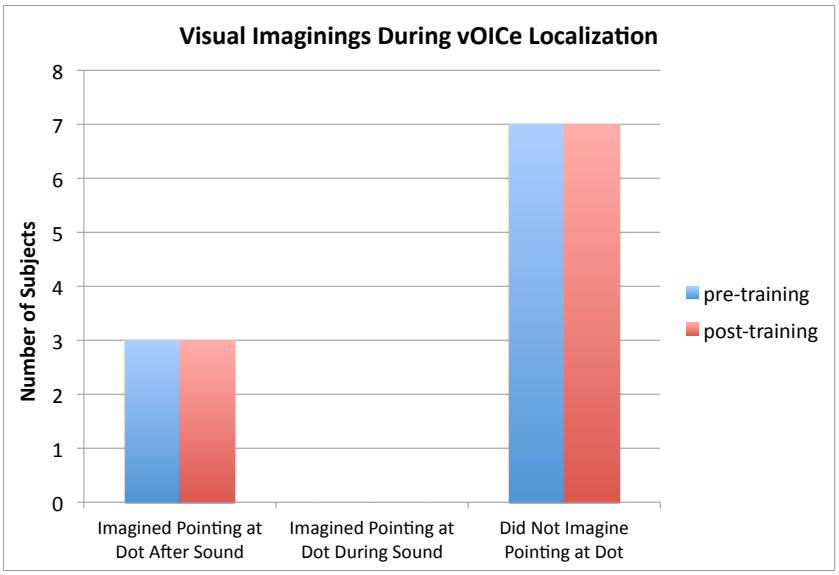

B

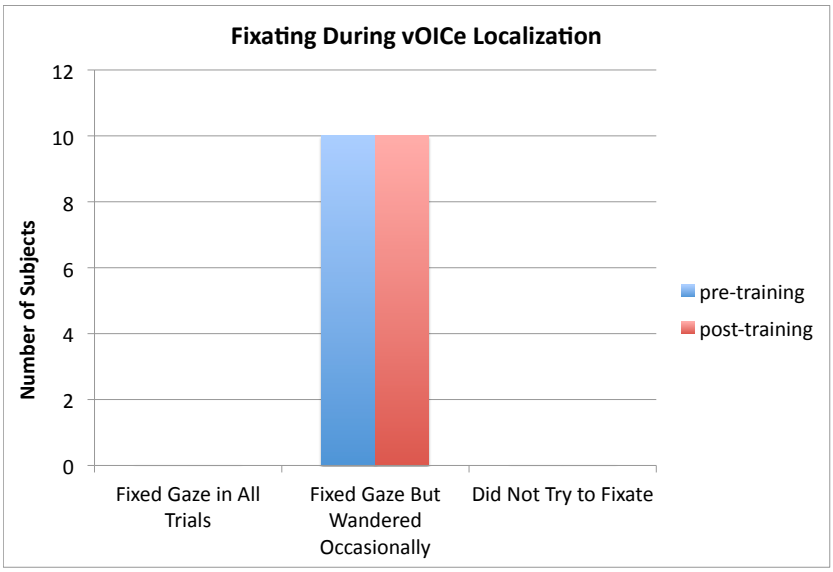

Figure 5.7. Post-experiment questionaire results. Following the post-training fMRI scan, all participants filled out a questionaire (Appendix C). This figure plots the responses to select questions in that questionaire for the 10 sighted participants.

Sighted Participants (*N* = 10)						
Region	BA	Side	*x*	*y*	*z*	p_{uncorr}
vOICe [Right – Left] Post Localization Slope Covariate						
Medial Frontal Gyrus	6	L	−3	32	37	0.000
vOICe [Right – Left] Post Localization Intercept Covariate						
Parahippocampal Gyrus	19	L	−30	−49	1	0.001
- small volume-corrected peak						0.035*
Culmen, Cerebellum		L	−6	−58	1	0.003

Table 5.3. fMRI covariate data: vOICe dot [Right – Left location] post-scan sighted participants. Two covariates for vOICe dot [Right – Left location] post-scan are displayed in this table, both based on vOICe training performance. Details on the processing of covariates is in the methods section and the results section of Chapter 4 (same covariates as last two in Table 4.4). The visual neural activation shown for the vOICe dot [Right – Left location] post-scan correlates with the performance metric, indicating that the covariate may have played a role in generating the neural activation listed. Brodmann Area localization was performed on the talaraich client for nearest grey matter. Any clusters without nearest grey matter within +/− 5 mm are not included. The small volume correction was for a sphere of 10 millimeter radius around the cluster center, and the pvalue shown (indicated by asterisk, *i.e.*, *) is for the peak level FWE-corrected.

Visually Impaired Neural Imaging Results

Four visually-impaired individuals performed the vOICe localization experiment: a severe low-vision participant, a late blind participant, and two congenitally blind participants (details on participants is in Chapter 4 methods, p. 130). The severe low-vision participant did not have any neural activation to the localization contrasts used (*i.e.* vOICe dot post [Right – Left location] or vOICe dot post [Left – Right location]). The results for the late blind participant and the congenitally blind participants are presented in Figure 5.8 and Table 5.4. The late blind participant ($N = 1$) had visual activation (BA 19, and 18) for the vOICe dot Post [Left – Right] in the right and left hemisphere (no activation for vOICe dot Post [Right – Left]). This is a bilateral mapping from visual space (left dot) to neural activation (right and left hemisphere). The first congenitally blind participant, WB, had quite different results: visual actvation (BA 17 and 18) for vOICe dot Post [Right – Left] in the right hemisphere. The congenitally blind participant WB, therefore has an ipsilateral mapping from visual space (right dot) to visual neural activation (right hemisphere). The second congenitally blind participant, SB, had visual activation (BA 19) for the vOICe dot Post [Left – Right] in the left and right hemisphere. Therefore, SB had a bilateral mapping of vOICe crossmodal plasticity. The sighted participants' ($N = 10$) results reported earlier for vOICe dot localization post-training (Table 5.1) had a contralateral mapping from visual space to neural activation. Therefore, interestingly, the sighted participants had a contralateral mapping, the late blind participant had a bilateral mapping, and the congenitally blind participants had an ipsilateral and bilateral mapping. Although there are too few blind participants (N = 2) to make strong conclusions, there is a trend for visual experience to be associated with a

contralateral mapping via vOICe, and lack of visual experience to be associated with an ipsilateral or bilateral mapping via vOICe.

A

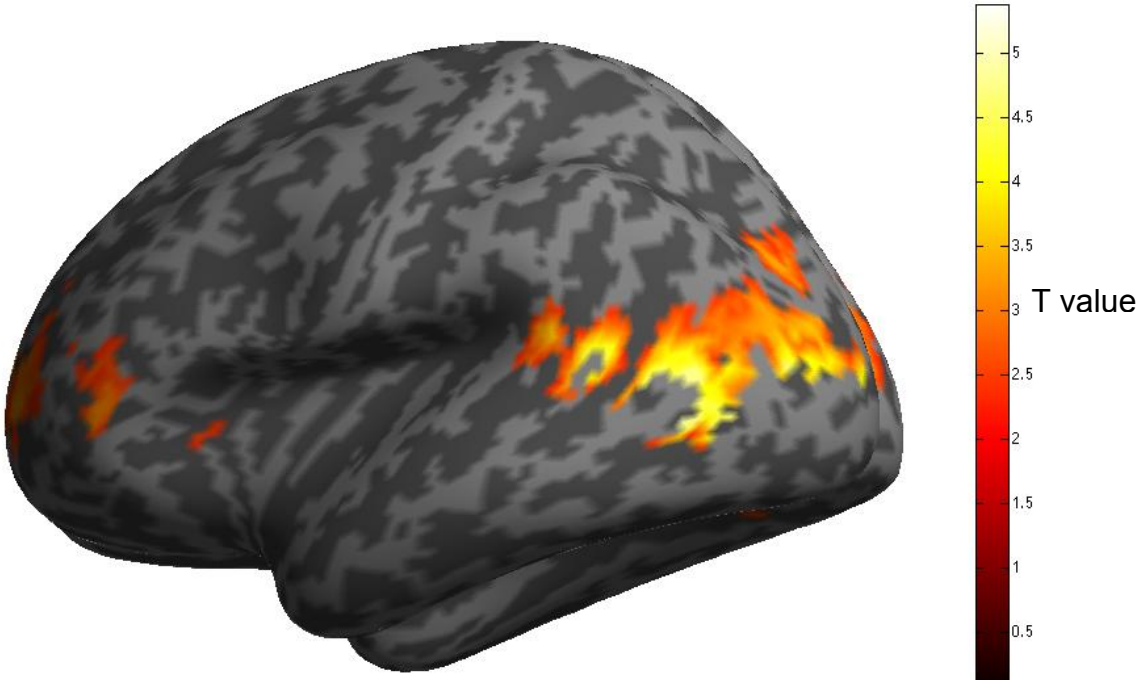

Figure 5.8. fMRI imaging results: vOICe dot [Right – Left location] post-scan congenitally blind participant ($N = 1$). The neural imaging result is displayed for the post-vOICe-training right dot in contrast to the post-vOICe-training left dot, both presented in vOICe with a blind participant ($N = 1$). Imaging data presented is $p < 0.009$ uncorrected and clusters of 10 voxels or more; further correction for multiple comparisons is shown in Table 5.4. Methods for fMRI data display are in the Chapter 4 methods. A severe low-vision participant ($N = 1$) also performed this experiment, but had no significant neural activation for this contrast.

A

Late Blind Participants (*N* = 1) (RD)						
Region	BA	Side	*x*	*y*	*z*	p_{uncorr}
vOICe Dot Post [Right – Left]						
No Activation						
vOICe Dot Post [Left – Right]						
Fusiform Gyrus	37	R	42	−55	−8	0.000
- small volume-corrected peak						0.000*
Claustrum			36	−22	−2	0.000
Fusiform Gyrus	19	R	42	−73	−11	0.000
- small volume-corrected peak						0.012*
Temporal Lobe	37	L	−42	−46	−8	0.000
Culmen		L	−18	−58	−8	0.000
Culmen		L	−21	−49	−11	0.000
Cuneus	18	R	15	−67	16	0.000
- small volume-corrected peak						0.003*
Posterior Cingulate	30	R	15	−52	13	0.000
Cuneus	18	R	12	−76	25	0.000
Middle Temporal Gyrus	39	R	51	−76	25	0.000
- small volume-corrected peak						0.007*
Middle Temporal Gyrus	39	R	57	−67	25	0.000
Middle Temporal Gyrus	39	R	60	−64	13	0.003
Middle Occipital Gyrus	18	L	−24	−82	−8	0.000
Thalamus		L	−3	−7	10	0.000
Lentiform Nucleus		L	−18	2	10	0.002

B

Congenitally Blind Participants (*N* = 1) (WB)						
Region	BA	Side	*x*	*y*	*z*	p_{uncorr}
vOICe Dot Post [Right – Left]						
Lingual Gyrus	17	R	18	−88	4	0.000
- small volume-corrected peak						0.000*
Lingual Gyrus	17	R	6	−85	4	0.000
Middle Occipital Gyrus	18	R	30	−79	1	0.000
- small volume-corrected peak						0.000*
Medial Frontal Gyrus	10	R	15	50	7	0.000
Medial Frontal Gyrus	10	L	−9	47	4	0.000
Medial Frontal Gyrus	10	R	18	68	4	0.000
vOICe Dot Post [Left – Right]						
Thalamus		L	−21	−16	10	0.000
Thalamus, Medial Dorsal Nucleus		L	−6	−13	4	0.001
Thalamus		R	24	−25	10	0.000

C

Congenitally Blind Participants (*N* = 1) (SB)						
Region	BA	Side	*x*	*y*	*z*	p_{uncorr}
vOICe Dot Post [Right – Left]						
No Activation						
vOICe Dot Post [Left – Right]						
Postcentral Gyrus	3	R	42	–25	61	0.000
Superior Frontal Gyrus	6	R	9	–16	61	0.000
Medial Frontal Gyrus	6	R	12	–28	58	0.000
Supramarginal Gyrus	40	R	60	–58	34	0.000
- small volume-corrected peak						0.000*
Inferior Parietal Lobule	40	R	66	–40	40	0.000
Middle Temporal Gyrus	39	R	54	–70	28	0.000
- small volume-corrected peak						0.002*
Precuneus	19	R	3	–88	46	0.000
- small volume-corrected peak						0.009*
Cuneus	19	R	12	–76	34	0.002
Cuneus	18	R	18	–79	25	0.004
- small volume-corrected peak						0.058*
Superior Temporal Gyrus	42	L	–60	–25	13	0.001
Postcentral Gyrus	43	L	–54	–7	19	0.001
Transverse Temporal Gyrus	42	L	–60	–16	16	0.001
Inferior Parietal Lobule	40	L	–63	–46	43	0.001
Precuneus	19	L	–42	–82	40	0.001
Angular Gyrus	39	L	–54	–70	40	0.001
Precuneus	19	L	–45	–76	46	0.001
Superior Temporal Gyrus	41	L	–42	–40	7	0.003

Congenitally Blind Participants (*N* = 1) (SB)						
Region	BA	Side	*x*	*y*	*z*	p_{uncorr}
Superior Temporal Gyrus	41	L	–42	–40	7	0.003
Superior Temporal Gyrus	41	L	–45	–31	10	0.004
Postcentral Gyrus	2	L	–39	–28	34	0.003
Cingulate Gyrus	31	R	24	–49	31	0.005

Table 5.4. fMRI data: vOICe dot [Right – Left location] post-scan blind participants. Select imaging results for blind participants when comparing the post-training left dot and the post-training right dot in vOICe ($N = 1$ for late blind and $\underline{N} = 1$ for congenitally blind). For the late blind participant, only the top 15 clusters of activation are presented in Panel A; a full list is in Appendix D, Table C. All other participant sub-tables contain a full list of neural activation. All regions were limited to $p < 0.009$ uncorrected and 10 voxel cluster threshold. The small volume correction was for a sphere of 10 millimeter radius around the cluster center, and the pvalue shown (indicated by asterisk, *i.e.*, *) is for the peak level FWE-corrected. Brodmann Area localization was performed on the talaraich client for nearest grey matter. Any clusters without nearest grey matter within +/– 5 mm are not included. A severe low-vision participant ($N = 1$) also performed this experiment, but had no significant neural activation for this contrast.

Discussion

This chapter focused on testing the topographical mapping of sensory substitution perception. The main experiment used the localization of a dot in the left or right visual field encoded into sound to determine whether it is contralaterally mapped like vision (*i.e.,* left dot activates right visual regions). This main experiment showed that after the vOICe training, visual region V3 was activated contralaterally for the vOICe right dot (*i.e.,* left hemisphere), but that this mapping was not present for the vOICe left dot. In fact, no visual activation occurred more strongly for the vOICe left dot when compared to the right dot encoded with vOICe. Interestingly, after training, a similar pattern occurred in the visual control (images of the dots were used rather than the sounds). The activation in left visual cortex may be due to dominance of the right side (hand dominance *etc*.) for most individuals, therefore making the left hemisphere more dominant. This localization task, which closely matches the localize, reach, and touch task in the office (detailed in Chapter 4 methods, Figure 4.07), may be engaging the left lateralized mirror system, which ranges from pre-motor, temporal and parietal regions (Ricciardi et al., 2009). In this case, the participants' motor mirror system would be mirroring a remembrance of performing the reach and touch task that they just performed in the lab outside the fMRI scanner 10 to 30 minutes before. While the topographic mapping does not entirely mimic normal vision's contralateral mapping, the visual control and vOICe sound were quite similar in scans following training, and it is possible that crossmodal plasticity from training caused this similarity between vision and vOICe mapping.

The post-training questionnaire was used to determine whether visualization played an important role in visual activation from vOICe sounds. The questionnaire showed that participants either visualized following the sound, or not at all. The scans used for analysis were during the vOICe sound; therefore, the contrasts did not capture any of the visualization by participants. This self-reporting evidence indicates that the visual activation from the vOICe task was not likely due to visualization by the participants. Further, a covariate analysis was used to determine whether any of the vOICe training performance correlated with the visual activation. The covariate for initial performance on vOICe (intercept) did correlate with visual activation in the vOICe task, indicating that the visual activation during the vOICe localization task was likely based on vOICe interpretation. This covariate is further evidence that it is the crossmodal interpretation of vOICe that originated the visual activation during the vOICe localization task.

The results from this chapter are not particularly definitive on the topographic mapping of vOICe sounds. The vOICe and vision mappings after vOICe training were similar but, unlike normal vision, strangely anisotropic. The fact that both vision and vOICe were asymmetrical may indicate that the localization task is too repetitive and simple, and therefore reducing visual activation. From another perspective, it could be the vOICe training itself that is impacting visual processing (as seen in Chapter 4). Just looking at the vOICe results, it is possible that more experience with vOICe is needed (than 5 hours of training) to generate a neurotypical contralateral mapping of space to visual activation. Perhaps an advanced user of sensory substitution would have a more solidified and consistent mapping generated from years of device use. In fact, the

echolocation spatial mapping of visual activation existed in an expert echolocator that had years of experience (Milne, et al., 2013). Therefore, these results likely indicate the beginning formation of a spatiotopic map of visual space with sensory substitution that is not yet fully complete.